PERGAMON

Journal of Structural Geology 25 (2003) 1241–1250

JOURNAL OF STRUCTURAL GEOLOGY

www.elsevier.com/locate/jsg

The control of stress history and flaw distribution on the evolution of polygonal fracture networks

G.W. Tuckwell[a,*], L. Lonergan[b], R.J.H. Jolly[b,1]

[a]*School of Earth Sciences and Geography, Keele University, Staffordshire ST5 5BG, UK*
[b]*Department of Earth Science & Engineering, Imperial College, Royal School of Mines, Prince Consort Road, London SW7 2BP, UK*

Received 12 January 2002; received in revised form 1 October 2002; accepted 9 October 2002

Abstract

We use boundary element models of fracture propagation and linkage to investigate the factors controlling the development of two-dimensional, multi-directional–polygonal fracture networks, characterised by a large number of abutting intersections between fractures. The position and orientation of a number of fracture seeds are prescribed in the model, which propagate when the applied stress reaches a critical value, according to linear elastic fracture mechanics theory. The applied boundary condition is a remote, isotropic, horizontal tension, where the stress is increased at a steady rate throughout each model to simulate continued fracture growth. Realistic polygonal systems are developed with the boundary element model simulations, which are comparable with those observed in natural systems (such as those found within Eocene and Oligocene mudrocks in the North Sea and on the surface of Mars). If conditions exist where a small number of fracture seeds propagate and develop significant structures before others, then these will dominate the resulting fracture network geometry. Not only do such early structures represent the largest fractures in the system, they also significantly modify the stress field around them preventing some other seeds from developing, and influencing the propagation paths of nearby fractures. Fracture seeding distribution and the rate at which the stress is increased are found to be the most significant parameters affecting the development of fracture network geometry. These results suggest that the geometry of evolving fracture networks should be considered not only in terms of the mechanical properties of the deforming material, but also in terms of the stress rate driving deformation.

Keywords: Polygonal fractures; Fracture growth; Numerical modelling; Stress; Tensile fracture

1. Introduction

An understanding of fracture geometry in two and three dimensions directly affects the geoscientist's ability to analyse subsurface fluid flow in fractured reservoirs, to model seismic wave propagation through fractured rock and to understand the evolution of geological structures. While outcrop exposures, or remotely sensed images of natural fault and fracture networks, provide snapshots of fracture systems in their final state, it is difficult to 'back track' and reconstruct fracture evolution from these data. A large body of rock mechanics and geological literature indicates that fracture network development is strongly controlled by the stress state that operated during formation, mechanical interactions between adjacent fractures, the material properties of the rock and local heterogeneities in the rock mass (e.g. Lawn and Wilshaw, 1975; Cotterell and Rice, 1980; Pollard et al., 1982; Atkinson, 1987; Germanovich et al., 1996 amongst many others). In some complex manner, it is the interplay of all of these factors that are responsible for the development of the resultant fracture pattern. Numerical models that incorporate these factors can be used to understand how fracture network geometries are related to the conditions of their formation. Here we report the results of numerical experiments using boundary element modelling based on linear elastic fracture mechanics to simulate the growth of two-dimensional polygonal fracture patterns. In particular we examine the role that stress history, flaw distributions in the rock mass, and material properties play in controlling the geometry of a fracture network as it grows.

Previous numerical work on the evolution of fracture systems has tended to concentrate on either linear fracture

* Corresponding author.
E-mail addresses: l.lonergan@ic.ac.uk (L. Lonergan), g.w.tuckwell@esci.keele.ac.uk (G.W. Tuckwell), jollr1@bp.com (R.J.H. Jolly).
[1] Now at: BP Exploration, Chertsey Road, Sunbury on Thames, Middlesex TW16 7LN, UK.

0191-8141/03/$ - see front matter © 2003 Elsevier Science Ltd. All rights reserved.
PII: S0191-8141(02)00165-7

systems (Cowie et al., 1993; Olson 1993; Renshaw and Pollard, 1994) or relatively simple intersecting en-échelon fracture geometries (Cowie, 1998; Olson and Pollard, 1989; Tuckwell et al., 1998). In this paper we investigate more complex two-dimensional fracture systems and model the growth and evolution of a network of fractures growing simultaneously, to form a polygonal pattern. Polygonal fracture systems occur on Earth from a centimetre to kilometre scale and have also been observed on the surface of Mars at a scale of tens of kilometres. Examples include the recently discovered polygonal faults that form within mudrocks at a kilometre scale in sedimentary basins (Cartwright and Lonergan, 1996; Lonergan et al., 1998; Watterson et al., 2000) and the giant polygons that have been imaged on the surface of Mars, in the Utopia Planita region (Carr et al., 1976; McGill, 1986; Hiesinger and Head, 2000; Fig. 1). The geological map of Utopia Planita suggests that the material deformed by the giant polygons is of volcanic, alluvial or aeolian origin (Greeley and Guest, 1987). The more recent work of Hiesinger and Head (2000) infers that the polygons occur in sediments of a paleolake that once filled the Utopia Basin. The principal geometrical characteristics of polygonal fracture sets are a lack of preferred fracture orientations, many more tip-to-wall type intersections than tip-to-tip linkages, and log-normal frequency/length distributions of fractures (Lonergan et al., 1998).

The tensile stresses required to generate polygonal fractures such as mudcracks, cooling joints in basalt, or permafrost polygons arise because the sediment or rock is prevented from contracting (Lachenbruch, 1962; Aydin and DeGraff, 1988). Similarly it has been suggested by Dewhurst et al. (1999) that polygonal fault arrays in North Sea mudrocks formed due to syneresis-induced contraction during burial. This process will result in an isotropic net tensional stress in all horizontal directions. Likewise the Martian polygons are attributed to cracking due to tension (see Hiesinger and Head (2000) for a recent review). Thus, as a first approach, a horizontal isotropic remote tension was applied as the loading condition in the numerical models to generate two-dimensional irregular polygonal fracture patterns. Undoubtedly in many natural polygonal systems additional stresses arising due to variations in temperature, layer thickness, slope and regional tectonic stresses will affect the resulting fracture patterns, but we do not include these effects in this work.

We were particularly interested in investigating the role that the build up of the remote loading stresses might have in influencing fracture growth. In polygonal systems, during continuing compaction, desiccation, or cooling the ambient tensile stresses will increase, and thus we examine the effect that building up this stress in large or small increments (to simulate fast and slow growth) has on the resultant polygonal fracture network. Mudcrack experiments show that the desiccation rate strongly influences the resultant fracture pattern. Large numbers of equi-dimensional cracks form simultaneously in thin mud layers that desiccate rapidly, whereas a thick mud layer that desiccates slowly is dominated by a few long cracks that are established early in the growth history (Corte and Higashi, 1964). Most previous

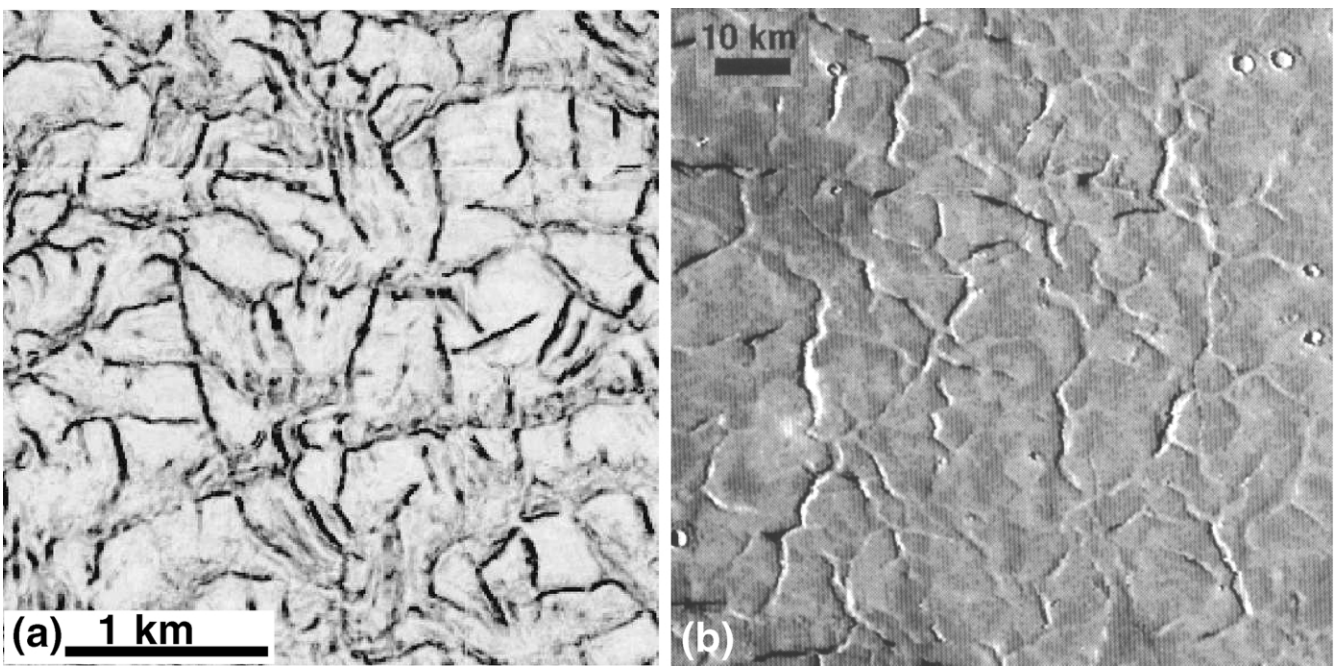

Fig. 1. Polygonal fracture sets: (a) an example of polygonal faults that form at a kilometre scale in mudrocks in the North Sea; coherence attribute map of part of an Upper Oligocene horizon in the Central North Sea, UK Quadrant 16, from a 3D seismic reflection dataset. (b) Viking orbiter image of polygonal terrain in Utopia Planita region, Northern Martian plains, at 230 m resolution (from Hiesinger and Head, 2000).

geological analyses of interacting fractures have not considered the effect of varying the rate at which the loading stress is applied (e.g. Olson, 1993; Cowie, 1998). Hence, the analysis described here, which is appropriate for polygonal systems, may also shed some further light on the growth of other fracture systems growing in response to stretching.

Experimental and theoretical work in elastic fracture mechanics suggests that fracture propagation rates in rocks are dependent on the energy at fracture tips (e.g. Atkinson, 1984; Olson, 1993). A fracture propagates once the stress intensity at the tip, K, exceeds a critical value known as the fracture toughness. For an isolated, two-dimensional crack tip, the stress intensity factor is a function of the remote loading stresses (σ_r), and the crack length, $2c$ (e.g. Lawn and Wilshaw, 1975; Atkinson, 1987):

$$K = \sigma_r(\pi c)^{1/2}, \tag{1}$$

and therefore for a single crack one would expect no difference in the resultant crack length whether the remote loading stress is applied in a few large increments or as many smaller increments. However, where a large number of fractures are growing simultaneously and mechanical interactions modify the local stress fields around neighbouring crack tips the situation becomes more complicated. The driving stress becomes a distribution that varies through the model area rather than a constant, and Eq. (1) no longer applies in this simple form.

2. Numerical method

A boundary element modelling code, based on the displacement discontinuity method of Crouch and Starfield (1990), is used to simulate the development of polygonal fracture systems. In this method, fractures are modelled by a series of short linear elements along each of which the relative displacement (e.g. opening and slip) is constant, and the resistance to shear stress is zero. In this way a system of fractures within a two-dimensional elastic medium can be described. The relative displacement of each boundary element, and the local stress field associated with the fracture system can be calculated given the elastic properties of the material, the far-field stress, and the stress boundary conditions on the fracture walls. In the model, individual fractures may grow by fracture propagation or linkage. Fracture propagation is simulated by the addition of a new element at the tip of a fracture. A fracture will propagate if the calculated stress intensity at the tip of the fracture exceeds the fracture toughness of the material (Lawn and Wilshaw, 1975). The mode I and II stress intensity factors, K_I and K_{II}, are calculated from the normal and shear displacement discontinuity of the tip element, D_n and D_s, by:

$$K_I = 0.806\left(\frac{\sqrt{\pi}E}{4(1-\nu^2)\sqrt{l}}\right)D_n,$$
$$K_{II} = 0.806\left(\frac{\sqrt{\pi}E}{4(1-\nu^2)\sqrt{l}}\right)D_s, \tag{2}$$

where E is Young's modulus, ν is Poisson's ratio, and l is the length of the fracture tip element (Olsen, 1991). The total stress intensity at the tip, K_{tip}, is calculated by (Lawn and Wilshaw, 1975):

$$K_{tip} = \cos\frac{\theta}{2}\left(K_I\cos^2\frac{\theta}{2} - \frac{3}{2}K_{II}\sin\theta\right). \tag{3}$$

The orientation of propagation, θ, is calculated such that the resolved normal stress on the new element is maximised (where tensile stresses are positive), and the resolved shear stress is zero, by:

$$K_I\sin\theta + K_{II}(3\cos\theta - 1) = 0 \tag{4}$$

(Erdogan and Sih, 1963).

The length of the new element is proportional to the magnitude of the stress intensity at the tip, which is the same criterion used by Renshaw and Pollard (1994) in their models of the evolution of a single, planar set of parallel fractures. In this way, fractures under greater driving stress than others will propagate faster, and the effect of stress history is explicitly built into the model. The second method of fracture growth is by linkage. This occurs by the interaction of process zones ahead of a propagating fracture. A process zone is defined as an area of micro-cracking and other non-linear deformation that occurs close to the fracture tip. The physical controls on the size of this zone are poorly understood (see Rubin (1993) for a review). Estimates for the size of process zones of shear faults are in the region of 10% of the fault length (e.g. Cox and Scholz, 1988; An and Sammis, 1996). Process zone size is likely to be less for mode I fractures, therefore we take this to be a maximum limiting value. We assume the extent of the process zone in our models is proportional to the stress intensity at the fracture tip, and that it can extend a maximum of 10% of the total fracture from the tip. Tip-to-tip linkage occurs in the model when the calculated extents of the process zone ahead of two propagating fractures overlap. In this event, new elements are created within the model joining the two tips. Tip-to-wall linkage will occur when the calculated extent of the process zone ahead of a propagating fracture overlaps the wall of another fracture. Stresses and displacements within the model are recalculated after each growth event.

A simple application of the numerical model to a pair of fractures is illustrated in Fig. 2. The two fractures are initiated by short seeds of equal length oriented parallel to the x-axis, with a relative offset in position in both x and y. A driving stress of 10 MPa is applied parallel to the y-axis. The

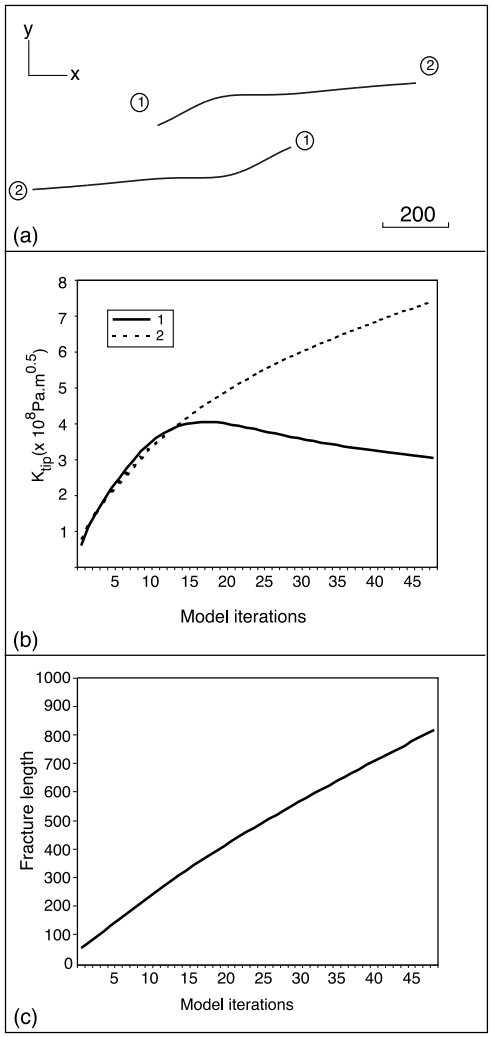

Fig. 2. Boundary element models of two propagating fractures in which the initial fracture seeds are equal in length (a). Graphs show the variation of stress intensity factor at fracture tips with model growth iteration (b) and fracture length against model growth iteration (c). Model length dimensions are arbitrary and are provided to facilitate a comparison with Fig. 3.

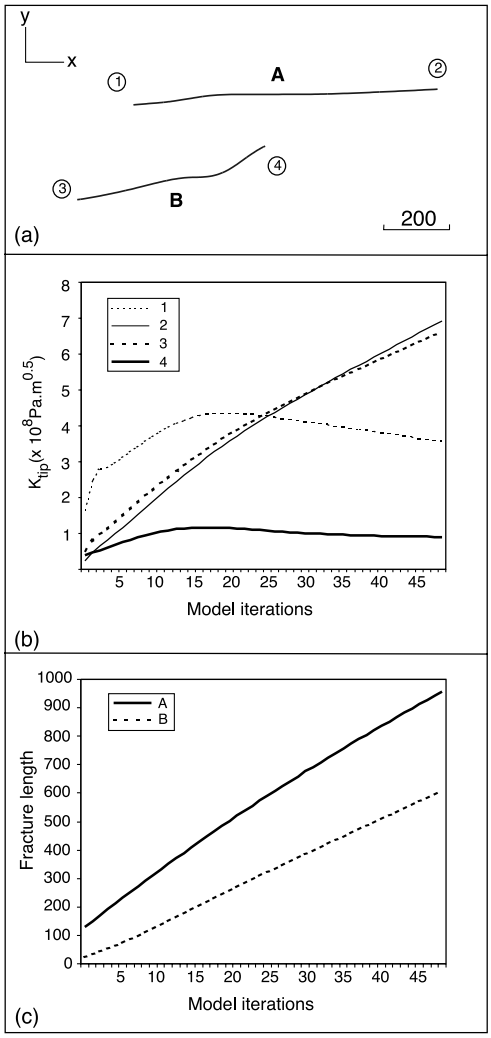

Fig. 3. Boundary element models of two propagating fractures in which the initial fracture seeds are unequal in length (a). Graphs show the variation of stress intensity factor at fracture tips with model growth iteration (b) and fracture length against model growth iteration (c). Model length dimensions are arbitrary and are provided to facilitate a comparison with Fig. 2.

model is symmetrical and the two fractures develop as mirrors of each other (Fig. 2a). Since the stress distribution in the models is recalculated after each growth iteration, mechanical interaction between fractures is implicit in the model formulation. Initially, the stress intensity factor at each tip is approximately equal (Fig. 2b). As the fractures propagate they begin to interact more strongly. This increased interaction is reflected both in the fracture propagation path and in the stress intensity factor at the tips. As tip 1 propagates it falls into the stress shadow of the other fracture and the stress intensity factor is reduced. As a result tip 2 will propagate at a greater relative velocity than tip 1. This experiment reproduces the results of Olson and Pollard (1989).

2.1. Varying fracture seed length

Next we investigate the asymmetric case where the initial seed for fracture A is five times the length of the initial seed for fracture B (Fig. 3). The starting position of the seeds and the driving stress are identical to those used in the symmetrical experiment. Because of the asymmetric fracture seed lengths, the stress intensity and propagation geometry are different at each fracture tip as the model evolves (Fig. 3b and c). Tip 1 has the highest stress intensity factor for the first half of the model run, and so propagates with a greater relative velocity during this period. In addition, there is relatively little deflection in the propagation path of this tip. Throughout the model run, the stress intensities at tips 2 and 3 are similar, but the propagation paths are different with tip 3 deflected to a greater extent from the *x*-axis. Tip 4 has the lowest stress intensity factor throughout the model, and the propagation path is greatly deflected towards the wall of fracture A. From the outset of the model, fracture A has an advantage over fracture B since it has a greater length. Consequently greater stress intensity

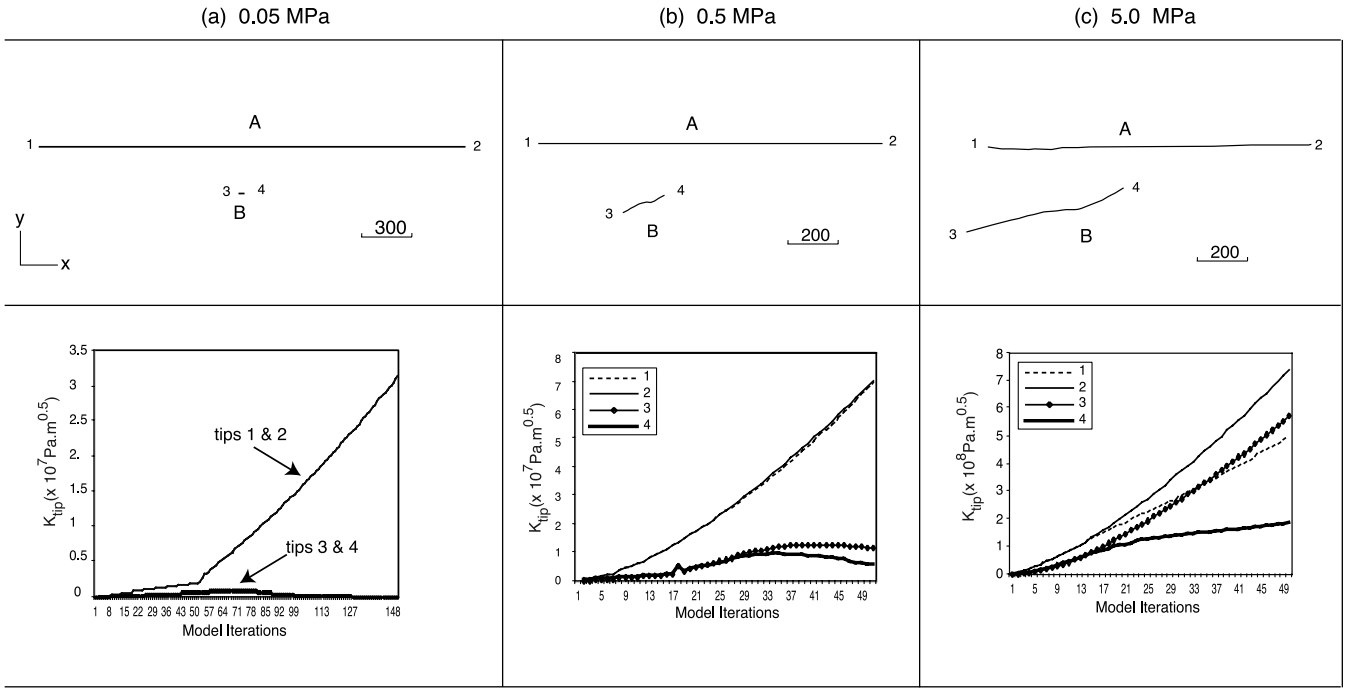

Fig. 4. Boundary element model of two propagating fractures, in which the seed length for fracture A was 10 times the length of the seed for B. Driving stresses in increments of 0.05 MPa were applied in model (a), 0.5 MPa in model (b) and 5 M Pa in model (c). Maps show the final fracture geometry at the end of the simulation. Graphs show the variation of stress intensity factor at fracture tips with model growth iteration. Model length dimensions are arbitrary and are provided to facilitate a comparison between the three simulations.

factors develop at the tips of fracture A than B, and fracture B remains shorter than fracture A (Fig. 3a and c). This positive feedback in mechanical advantage is a key property of interacting fractures. The larger fractures in the system will typically propagate at a greater relative rate, and will affect the growth of smaller fractures (compare Figs. 2c and 3c).

2.2. Varying size of stress increment

In a final simple example, we have repeated the asymmetric two-fracture experiment but varied the size of the stress increment applied between each model step by factors of 10 (Fig. 4). As in the experiment illustrated in Fig. 3, the two seeds are oriented parallel to the x-axis, with a relative offset in position in both x and y, but fracture A started out with an initial seed that was 10 times the length of B. A driving stress in increments of 0.05, 0.5 and 5 MPa, respectively, was applied parallel to the y-axis. The results of these model runs particularly emphasize the control that the magnitude of the driving stress, and thus different loading histories, has on the final fracture geometry. At lower rates of stress increase (Fig. 4a and b), the stress intensities at the tips of fracture A increase much more rapidly than the tips of B, and thus fracture A propagates more quickly and becomes longer during the model run. At higher rates of stress increase there is less of a difference between the stress intensities at the tips of fracture A, and tip 3 on fracture B and consequently fracture B can grow more rapidly than it could when smaller stress increments were applied (Fig. 4c). Thus, decreasing the size of the stress increment between model steps amplifies the mechanical advantage of the longer fractures in the system.

3. Models of polygonal fracture networks

To model the development of polygonal fracture networks, we begin with a set of 50 fracture seeds in a square area of dimensionless area L^2. The seeds represent flaws in the original rock, from which a fracture can propagate. In order to assess the dependence of the models on the spatial distribution of seeds, two end-member distributions are used: a random distribution, and a regular, equally spaced arrangement of seeds. Two distributions of initial seed lengths were used. Since the stress intensity at the fracture tips is related to length (Eq. (1)), and propagation occurs when the stress intensity exceeds the fracture toughness of the material, fracture seeds of different lengths can be considered to represent flaws of different strengths. Therefore a greater range of initial seed lengths represents a more heterogeneous material. Seed lengths either varied randomly between 0 and $0.001L$, or between $0.0004L$ and $0.0006L$. Hereafter we distinguish these as high and low heterogeneity. The fracture seeds are oriented randomly, and are sufficiently short and spaced widely enough that they induce only small local stress field perturbations so there is essentially no mechanical interaction between

Table 1
Main statistical characteristics of final fracture maps from the numerical models, and similar data for four polygonal fracture maps in mudrocks in the UK North Sea, for comparison (see Lonergan et al. (1998) for original data); Letters 'F/S, H/L, H/L' refer to fast/slow stress accumulation, high/low elastic strength, high/low material heterogeneity, respectively

	Four random seeds				Same starting seed, different model parameters						Regular seeds			North Sea data			
	FHH	FHH01	FHH02	FHH03	SHH	FHL	SHL	FLL	SLL	FLH	SLH	SHL_R	FHL_R	FHH_R	MAP A	MAP B	MAP C	MAP D
Orientation																		
Vector mean	60	135	123	123	86	53	94	52	103	69	88	87	94	95	142	42	88	32
Mean vector length (0–1)	0.12	0.12	0.04	0.13	0.03	0.04	0.09	0.06	0.11	0.15	0.016	0.07	0.06	0.04	0.151	0.12	0.027	0.178
Intersection types																		
Tip-to-tip	10%	18%	19%	14%	19%	6%	22%	7%	16%	17%	17%	9%	8%	14%	21%	31%	33%	39%
Tip-to-wall	75%	78%	76%	82%	76%	91%	74%	90%	71%	77%	72%	82%	89%	82%	61%	52%	43%	56%
Complex	15%	4%	5%	4%	5%	3%	4%	3%	13%	6%	11%	9%	3%	4%	17%	17%	24%	5%
Length distribution																		
Geometric mean	113.7	119.5	113	157	93	152.3	110	130	109	79	54	92	161	111.5	397 m	535 m	294 m	277 m

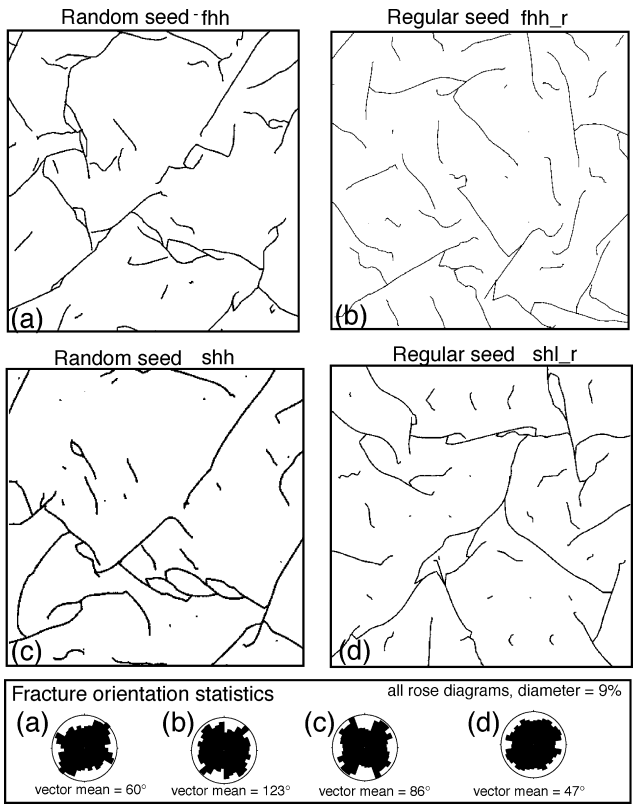

Fig. 5. Comparison of four final fracture models: (a) and (b) fast stress remote loading rate for models with random and regular initial fracture seeds, respectively; (c) and (d) slow stress loading rate for models with random and regular initial fracture seeds, respectively. Note how in the slow models a small number of long fractures dominate the final fracture map.

neighbouring seeds at the beginning of each simulation. As the model develops, fracture seeds begin to propagate as the stress intensities at their tips exceed the fracture toughness of the material. In our models, we define the initiation of seed growth as fracture nucleation. In addition to the heterogeneity of the material, the effects of two other parameters were investigated. Elastic moduli were chosen to bracket values typical of sedimentary rocks (Cripps and Taylor, 1981; Atkinson et al., 1990). Half the models were run with a Young's modulus, $E = 140$ MPa, and bulk modulus, $G = 75$ MPa. The other half were run with $E = 14$ MPa, and $G = 7.5$ MPa. These we term as elastically stiff and elastically compliant, respectively. The final parameter investigated was the loading history for the model. The stress applied to the models is increased incrementally from zero after each calculation step to simulate the accumulation of elastic strain. The model calculations include the local redistribution of this stress by brittle failure. Two different loading histories were used in the models, with stress increasing from zero by 0.5 or 0.05 MPa with each growth increment. These are referred to as fast and slow stress accumulation, respectively, and represent fast or slow shrinkage rates during polygonal fracture network evolution. The parameter combinations for

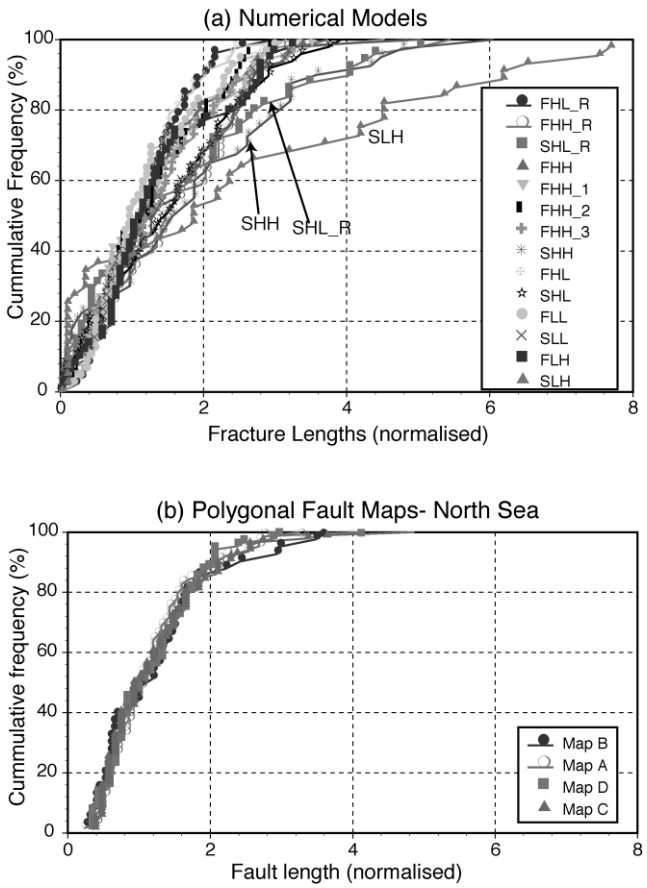

Fig. 6. Cumulative frequency plots of fracture lengths for numerical models and real data (polygonal faults in the North Sea; maps A–D refer to data in Fig. 4 of Lonergan et al. (1998)).

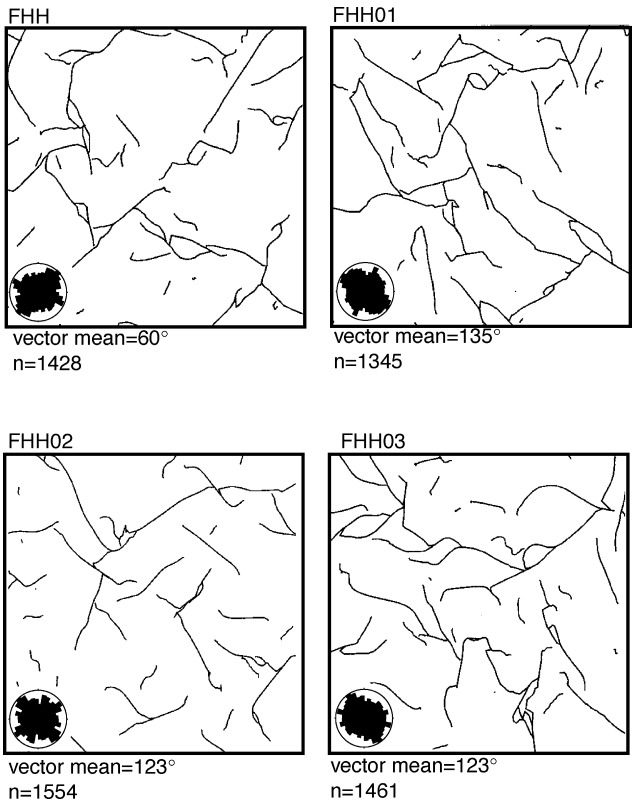

Fig. 7. Comparison of four final fracture models with four different initial random fracture seeds. Other mechanical properties were the same for each model, i.e. fast stress accumulation rate, elastically stiff material and high material heterogeneity (FHH).

each of the 14 simulations are identified by three letters, *ABC*, in Table 1 and Figs. 5–7. The value for *A* can be F or S and refers to a stress loading increment of 0.5 or 0.05 MPa; for *B* can be H or L referring to elastically stiff or compliant moduli and for *C* can be H or L indicating high or low material heterogeneity. Additionally a regular initial seed distribution is distinguished from a random seed distribution by the addition of a further suffix, '_R'.

4. Description of polygonal geometries

Numerical models were run for all combinations of elastic moduli, seed length distribution and loading history to investigate the effects of each parameter (Table 1). The model fracture arrays (Fig. 5) visually reproduce the main characteristics of other natural irregular polygonal fracture sets, such as those illustrated in Fig. 1, and are judged to be realistic representations of polygonally organized extensional fractures. A vector mean of the length-weighted fracture orientations was calculated for each simulation (Table 1, and rose diagrams in Figs. 5 and 7). The mean length of this vector, *L*, is a measure of the dispersion in the orientation data, with high values of *L* indicating that most of the fractures are tightly clustered about the mean. Conversely values of *L* close to zero imply that the data are dispersed. For both the numerical simulations and North Sea polygonal data, the values of *L* are close to zero (Table 1). Standard statistical tests for circular distributions (e.g. Von Mises distributions and the Rayleigh test; Cheeney, 1983; Davis, 1986) confirm that none of the calculated mean orientations are statistically different to the mean of a uniform circular distribution; i.e. there is no statistically significant preferred fracture orientation.

An analysis of linkage types shows a majority of tip-to-wall linkages over tip-to-tip linkages and intersections of more than two fractures (labelled complex intersections in Table 1) and the fracture lengths have log-normal length frequency distributions (Fig. 6). For the majority of the numerical model simulations the fracture length distributions, when normalised to the geometric mean, are indistinguishable from North Sea polygonal datasets (Fig. 6). All numerical realisations show features typical of mechanical interaction between propagating cracks, with fracture tips curving in towards neighbouring fractures.

For the same initial fracture seed distributions, different mechanical conditions generate strikingly different fracture patterns, and from the final maps it would be impossible to deduce that the fracture patterns grew from the same initial distribution of flaws (compare maps *a* and *c* with same random flaw distribution; and maps *b* and *d* with same regular flaw distribution in Fig. 5). Of the mechanical variables tested in the 14 simulations, the rate of stress increase (large or small increments during the model evolution) was the most significant parameter affecting the development of the fracture network geometry. Of the 14 different simulations, five were run with a slow stress accumulation loading history (SHH, SHL, SLL, SLH and SHL_R in Table 1). Three of these are distinguishable on the length frequency graph (Fig. 6), as they have higher relative proportions of longer fractures, compared with all other simulations. Within the range of values tested, variation in elastic moduli, and material heterogeneity have the least affect on the final fracture geometry. When the mechanical conditions are held constant, the heterogeneity introduced by either random or regular initial seed distributions produces very different final network geometries (compare maps *a* and *b*, model FHH with FHH_R; Fig. 5). When different random starting seed distributions are used, again the resultant fracture network geometries are markedly different (Fig. 6).

5. Fracture network evolution—effect of stress history, flaw distribution and material properties

The ability to examine the fracture network as it evolves helps to provide insights as to why both the rate of stress accumulation and the distribution of the initial fracture nucleation loci exert such a strong control on the final network geometry (Fig. 8). Visual differences in fracture patterns grown from exactly the same seed distribution can be attributed to the early development of a small number of fractures. Larger fractures will typically propagate at a greater relative rate within the model. Thus if a long fracture

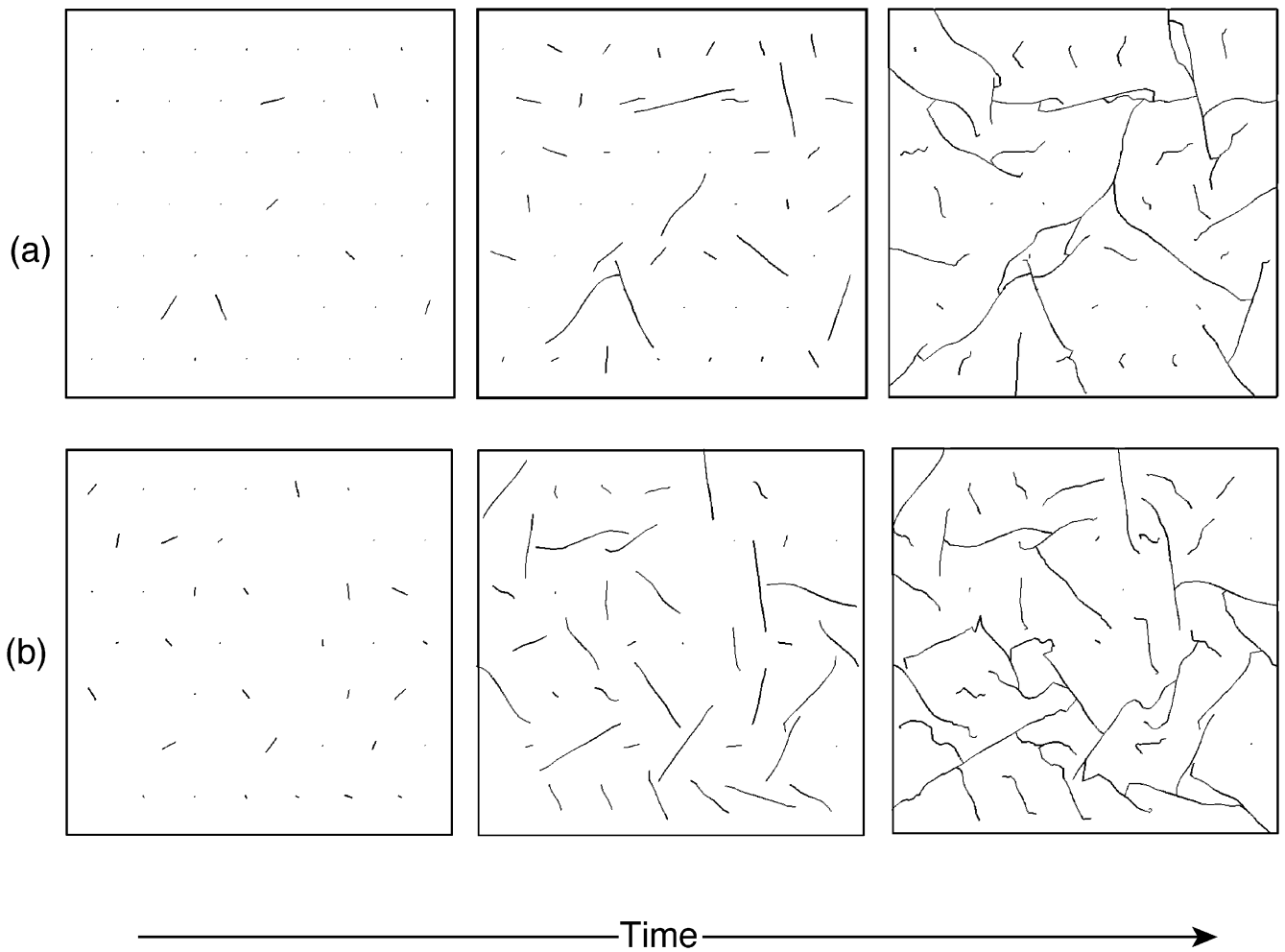

Fig. 8. Evolution of a polygonal fracture network using the boundary element simulation: (a) slow stress accumulation rate; (b) fast stress accumulation rate. Model (a) is run SHL_R (elastically stiff material with low heterogeneity); model (b) is run FHH_R (elastically stiff material with high heterogeneity). A regular starting seed distribution was used for the two simulations.

develops early in the model a positive feedback mechanism promotes its growth relative to others. If conditions exist within the model such that a small number of randomly oriented fractures begin to propagate early in the development of the fracture network, then these fractures go on to strongly influence the subsequent development of the network (Fig. 8a). A small number of long fractures developed early in the model run will dominate the local stress field, and as subsequent fractures develop and grow, their propagation paths are strongly influenced by the large fractures. Fractures developing later in the models tend to propagate at high angles to the pre-existing fractures. The final fracture pattern produced may appear visually to have some preferred fracture orientations (see most evolved map in Fig. 8a—final state of model SHL_R), although statistically there is no significant orientation (Table 1). Conversely, if the majority of fractures begin to propagate at the same time (Fig. 8b), no single or small sub-set of fractures dominates the stress field, and the fracture network developed appears to be more uniform. Such a model develops a narrower range of fracture lengths, with proportionally fewer short fractures.

The early development of a small number of fractures is associated with (1) a slow loading history and (2) an elastically compliant material with high heterogeneity. Of these two factors, slow loading history appears to exert the greatest control. A heterogeneous material will contain a small number of relatively large fracture seeds, equivalent to a small number of relatively weak areas within the material. As the loading stress increases, these seeds begin to propagate before others within the model. A more heterogeneous material promotes the early development of a small number of fractures. In our tests, the rate of increase of the loading stress was found to have the greatest effect on the geometry of the evolved fracture network. Consider an applied loading stress sufficient for a small number of fractures to begin to propagate. If this loading stress is increased rapidly, then other fracture seeds within the model begin to propagate before the early fractures have increased in length. However, if the loading stress is such that only a small number of fractures will propagate, and remains so long enough for these fractures to increase significantly in length, they will dominate the model regardless of subsequent stress changes.

6. Conclusions

The process of recreating natural fracture patterns using numerical simulation based on a few mechanical rules provides a valuable insight into the controlling influences on polygonal fracture network development. We have successfully used boundary element models of fracture growth and linkage to reproduce polygonally organized fracture patterns, such as those that occur in mudrocks in the North Sea and on the surface of Mars. Our results show that the detailed geometry of the fracture network is greatly affected by the early stress history during fracture nucleation. In a heterogeneous material, a slow accumulation of far-field stress favours early development of a small number of fractures. These early fractures modify the local stress field, and influence the propagation path of the fractures around them. The positive feedback during growth can cause small differences in initial growth to produce long fractures, which have a very significant effect on the resultant fracture pattern. Here, we have used only a limited range of possible stress histories as boundary conditions for the models. Sharp changes in stress conditions have not been considered nor has the possibility that for many polygonal fracture systems the rate of increase of driving stresses may start out high and then decrease. For example, in systems that are cooling or desiccating the rate of tensile stress increase may be highest early on when cooling or desiccation rates are greatest.

These experiments are based on opening mode fracturing, for a case of idealistic linear elastic fracture mechanics. However, the key property controlling model behaviour is the positive feedback that favours the development of longer fractures. This feedback operates in other tectonic fault systems (e.g. Pollard and Segall, 1987) and has been observed in numerical simulations of linear fracture arrays (Olson, 1993; Renshaw and Pollard, 1994). If the results presented here can be extrapolated to other structural settings, then there may be significant implications for other models of fault growth and interaction, which do not incorporate the effects of stress history dependency on final geometries.

Acknowledgements

We thank S. Martel and R. Bürgmann for detailed and very helpful comments on a previous version of this manuscript that led to significant improvements, D.A. Ferrill for further comments, and D. Sanderson, D. Pollard and J. Olson for helpful discussions during the course of this work. LL is funded by the Royal Society; RJHJ was funded by a NERC ROPA award.

References

An, L.-J., Sammis, C.G., 1996. A cellular automation for the development of crustal shear zones. Tectonophysics 253, 247–270.

Atkinson, B.K., 1984. Subcritical crack growth in geological materials. Journal of Geophysical Research 89, 4077–4114.

Atkinson, B.K., 1987. Fracture Mechanics of Rocks, Academic Press, London.

Atkinson, J.H., Richardson, D., Stallebrass, S.E., 1990. Effect of recent stress history on the stiffness of overconsolidated soil. Geotechnique 40, 531–540.

Aydin, A., DeGraff, J.M., 1988. Evolution of polygonal fracture patterns in lava flows. Science 239, 471–476.

Carr, M.H., et al., 1976. Preliminary results from the Viking orbiter imaging experiment. Science 193, 766–776.

Cartwright, J.A., Lonergan, L., 1996. Volumetric contraction during the compaction of mudrocks: a mechanism for the development of regional-scale polygonal fault systems. Basin Research 8, 183–193.

Cheeney, R.F., 1983. Statistical Methods in Geology, George Allen & Unwin, London.

Corte, A.E., Higashi, A., 1964. Experimental research on desiccation cracks in soil. Research Report—Corps of Engineers, U.S. Army, Cold Regions Research and Engineering Laboratory, pp. 1–76.

Cotterell, B., Rice, J.R., 1980. Slightly curved or kinked cracks. International Journal of Fracture 16, 155–169.

Cowie, P.A., 1998. A healing-reloading feedback control on the growth rate of seismogenic faults. Journal of Structural Geology 20, 1075–1087.

Cowie, P.A., Vanneste, C., Sornette, D., 1993. Statistical physics models for the spatiotemporal evolution of faults. Journal of Geophysical Research 98, 21809–21821.

Cox, S.J.D., Scholz, C.H., 1988. Rupture initiation in shear fracture of rocks; an experimental study. Journal of Geophysical Research 93, 3307–3320.

Cripps, J.C., Taylor, R.K., 1981. The engineering properties of mudrocks. Quarterly Journal of Engineering Geology London 14, 325–346.

Crouch, S.L., Starfield, A.M., 1990. Boundary Element Methods in Solid Mechanics, Unwin, Hyman, Boston, MA.

Davis, J.C., 1986. Statistics and Data Analysis in Geology, 2nd ed, Wiley, New York.

Dewhurst, D.N., Cartwright, J.A., Lonergan, L., 1999. The development of polygonal fault systems by syneresis of colloidal sediments. Marine and Petroleum Geology 16, 793–810.

Erdogan, F., Sih, G.C., 1963. On the crack extension in plates under plane loading and transverse shear. Transactions of the American Association of Mechanical Engineers 85, 519–527.

Germanovich, L.N., Carter, B.J., Ingraffea, A.R., Dyskin, A.V., Lee, K.K., 1996. Mechanics of 3-D crack growth under compressive loads. In: Aubertin, M., Hassani, F., Mitri, H.S. (Eds.), Rock Mechanics. Proceeding of 2nd North American Rock Mechanics Symposium, Balkema, Rotterdam, pp. 1151–1160.

Greeley R., Guest, J.E., 1987. Geologic map of the eastern equatorial region of Mars 1:15,000,000. U.S. Geological Survey Miscellaneous Investigation Series. Map 1-1802-B.

Hiesinger, H., Head, J.W. III, 2000. Characteristics and origin of polygonal terrain in southern Utopia Planitia, Mars: results from Mars Orbiter Laser Altimeter and Mars Orbiter Camera Data. Journal of Geophysical Research-Planets 105, 11999–12022.

Lachenbruch, A.H., 1962. Mechanics of thermal contraction cracks and ice-wedge polygons in permafrost. Geological Society of America Special Paper 70, 69pp.

Lawn, B.R., Wilshaw, T.R., 1975. Fracture of Brittle Solids, Cambridge University Press, New York.

Lonergan, L., Cartwright, J., Jolly, R., 1998. The geometry of polygonal fault systems in Tertiary mudrocks of the North Sea. Journal of Structural Geology 20, 529–548.

McGill, G.E., 1986. The giant polygons of Utopia, northern Martian plains. Geophysical Research Letters 13, 705–708.

Olsen, J., 1991. Fracture mechanics of joints and veins. Ph.D. dissertation, Stanford University.

Olson, J., 1993. Joint pattern development: effects of subcritical crack growth and mechanical crack interaction. Journal of Geophysical Research 98, 12,251–12,265.

Olson, J., Pollard, D.D., 1989. Inferring paleostresses from natural fracture patterns: a new method. Geology 17, 345–348.

Pollard, D.D., Segall, P., 1987. Theoretical displacements and stresses near fractures in rock: with applications to fault, joints, veins, dykes and solution surfaces. In: Atkinson, B.K., (Ed.), Fracture Mechanics of Rock, Academic Press, San Diego, CA, pp. 277–350.

Pollard, D.D., Segall, P., Delaney, P.T., 1982. Formation and interpretation of dilatant échelon cracks. Geological Society of America Bulletin 93, 1291–1303.

Renshaw, C.E., Pollard, D.D., 1994. Numerical simulation of fracture set formation: a fracture mechanics model consistent with experimental observations. Journal of Geophysical Research 99, 9359–9372.

Rubin, A.M., 1993. Tensile fracture of rock at high confining pressure: implications for dike propagation. Journal of Geophysical Research 98, 15,919–15,935.

Tuckwell, G.W., Bull, J.M., Sanderson, D.J., 1998. Numerical models of faulting at oblique spreading centers. Journal of Geophysical Research 103, 15,473–15,482.

Watterson, J., Walsh, J.J., Nicol, A., Nell, P.A.R., Bretan, P.G., 2000. Geometry and origin of a polygonal fault system. Journal of the Geological Society (London) 157, 151–162.